

# Transcription and noise in negative feedback loops

J.C. Nacher<sup>1</sup> and T. Ochiai<sup>2</sup>

February 15, 2013

<sup>1</sup> *Department of Complex Systems, Future University-Hakodate*

*116-2 Kamedankano Hakodate, Hokkaido, 041-8655, Japan*

nacher@fun.ac.jp

<sup>2</sup> *Faculty of Engineering, Toyama Prefectural University*

*5180 Kurokawa Imizu-shi Toyama, 939-0398, Japan*

ochiai@pu-toyama.ac.jp

PACS number : 87.14.Ee, 87.14.Gg, 87.15.Aa, 87.15.Ya,

Keywords : Autoregulatory genetic module, Stochastic theory, Noise, Fokker-Planck equation.

## Abstract

Recently, several studies have investigated the transcription process associated to specific genetic regulatory networks. In this work, we present a stochastic approach for analyzing the dynamics and effect of negative feedback loops (FBL) on the transcriptional noise. First, our analysis allows us to identify a bimodal activity depending of the strength of self-repression coupling  $D$ . In the strong coupling region  $D \gg 1$ , the variance of the transcriptional noise is found to be reduced a 28 % more than described earlier. Secondly, the contribution of the noise effect to the abundance of regulating protein

becomes manifest when the coefficient of variation is computed. In the strong coupling region, this coefficient is found to be independent of all parameters and in fair agreement with the experimentally observed values. Finally, our analysis reveals that the regulating protein is significantly induced by the intrinsic and external noise in the strong coupling region. In short, it indicates that the existence of inherent noise in FBL makes it possible to produce a basal amount of proteins even though the repression level  $D$  is very strong.

## 1 Introduction

The cell is a highly dynamic and regulated system composed of complex pathways and networks formed by tens thousands of inter-connected proteins, genes, and metabolites. Gene expression regulation is a complex cellular process that involves different genetic elements, through which cells control multiple functions such as the synthesis of mRNA molecules and the production of enzymatic proteins. Recently, it has been shown that stochastic fluctuations in populations of genetic and biochemical molecules can influence the gene regulatory processes [1, 2, 3]. Each cell represents a complex system that has evolved in the presence of considerable variations and random fluctuations of molecular components. As a consequence, cells have been adapted to exploit the noise to enhance cellular processes [4, 5, 6, 7, 8, 9, 10].

In the transcriptional process, a part of DNA sequence (gene) is copied by an RNA polymerase to synthesize mRNA molecule. In a second step, mRNA is decoded to produce specific gene products like transcriptional factors (TF) or proteins. This transcriptional process can be affected by two sources of noise. While the internal noise emerges from low copy number of molecules and the random encounters between reactants, the external noise is related to changes in the neighborhood and environmental conditions [2, 6].

One mechanism that the cell uses to deal with noise is the negative feedback loop (FBL) [11]. Both theoretical and experimental studies on a FBL in *Escherichia coli* showed that these auto-regulatory genetic modules decrease transcriptional noise and enhance the stability in genetic networks [6, 8, 12, 13]. Furthermore, the propagation of noise in genetic networks is a further interesting question [14, 15]. However, challenges still remain to obtain a more accurate description of the transcriptional process governed by negative feedback loops.

In this paper, we study the auto-regulatory genetic module using a stochastic model. The original work that experimentally and theoretically analyzed this module was shown in [12]. We first derive the potential and the gene product probability distributions corresponding to the auto-regulatory module. We then evaluate the role of noise by computing the expectation and variance values. We show that our approach leads to new insights into the FBL. We were able to characterize the system according to two different phases: weak and strong feedback regions. In particular, our model predicts that the FBL decreases noise in the strong coupling region a 28 % more than described earlier [12]. Furthermore, we obtained a coefficient of variation of 0.75 in the strong coupling region, which is independent of all parameters. Remarkably, this predicted value is in agreement with the experimental value observed in [16].

The paper is organized as follows. First, we describe the formulation of our model. Next section shows the results classified in subsections corresponding to the potential, probability distribution, expectation value, variance and noise dependence. The last section discusses and summarizes our findings.

## 2 Stochastic model formulation

A deterministic model to study the auto-regulatory module was first introduced by [17]. The model was based on thermodynamic theory and kinetics associated to the system (see [17] for details). The RNA polymerase is possibly bound to the promoter and the protein is also bound to the operator site. Therefore, the single gene, single promoter and single operator site system has three different configurations. The first state ( $s=1$ ) is that neither the RNA polymerase nor protein are bounded to the promoter and the operator site, respectively. The second state ( $s=2$ ) is that the RNA polymerase is bound to the promoter, but the protein is not bound to the operator. The third state ( $s=3$ ) is that the RNA polymerase is not bound to the promoter, but the protein is bound to the operator. The state that both the RNA polymerase and protein are bound to the promoter and the operator site respectively is prohibited, since repressor protein prevents the RNA polymerase from attaching the promoter site. According to the model, the concentration  $x$  of unbounded regulating proteins obeys the following equation:

$$\frac{dx}{dt} = \frac{k\alpha e^{-\Delta G_2/RT} [RNAP]}{e^{-\Delta G_1/RT} + e^{-\Delta G_2/RT} [RNAP] + e^{-\Delta G_3/RT} x} - \lambda x, \quad (1)$$

where  $\Delta G_s$  is the Gibbs free energy of state  $s$ ,  $R$  is the gas constant,  $T$  is the absolute temperature,  $[RNAP]$  is the concentration of unbound RNA polymerase molecules,  $x$  is the concentration of unbounded regulating protein,  $k$  is the rate of RNA polymerase isomerization from closed to open complex,  $\alpha$  is the proportionality coefficient that represents the number of protein synthesized per complex formed, and  $\lambda$  is the protein degradation rate. To clarify the argument, we simplify equation (1) as follows:

$$\frac{dx}{dt} = \frac{A}{C + Dx} - \lambda x, \quad (2)$$

where  $A = k\alpha e^{-\Delta G_2/RT} [RNAP]$ ,  $C = e^{-\Delta G_1/RT} + e^{-\Delta G_2/RT} [RNAP]$ ,  $D = e^{-\Delta G_3/RT}$ .

By using a stochastic partial differential equation (SPDE), we can derive a stochastic regulatory model that allows us to include the stochastic nature of the transcriptional process. This can be done by replacing the usual variable  $x$  by the stochastic variable and adding the noise term in Eq. (1). As a result, the SPDE of one gene, one operator-site system is given by

$$dX_t = a(X_t)dt + \sigma dW_t, \quad (3)$$

where

$$a(X_t) = \frac{A}{C + DX_t} - \lambda X_t. \quad (4)$$

Here, the stochastic variable  $X_t$  denotes the fluctuating concentration of unbounded regulating protein,  $W_t$  corresponds to the Wiener process and  $\sigma$  represents the combined effect of internal and external noise.

### 3 Results

#### 3.1 Potential representation of the FBL

The potential of the system given by Eq. (3) can read as follows:

$$\begin{aligned} U(x) &= - \int^x a(s) ds \\ &= -\frac{A}{D} \log(C + Dx) + \frac{1}{2} \lambda x^2 \quad \left(x > -\frac{C}{D}\right). \end{aligned} \quad (5)$$

The strength of the coupling between the unbounded regulating proteins (also known as transcriptional factors) and the operator site is represented by the parameter  $D$ . Then, high  $D$  values indicate strong coupling probability. Then, FBL will strongly repressed the production of new regulating proteins. In the following, we analyze how is the shape of the potential in both weak and strong coupling regions.

**The weak coupling limit** In the weak feedback region  $D \rightarrow 0$ , the potential (5) takes the form:

$$U(x) = \frac{1}{2} \lambda \left(x - \frac{A}{\lambda C}\right)^2 - \frac{A^2}{2\lambda C^2} - \frac{A}{D} \log C \quad (6)$$

This is the classical Gaussian potential.

**The strong coupling limit** In the strong feedback region  $D \rightarrow \infty$ , the shape of the potential (5) is transformed into the following expression:

$$U(x) = \begin{cases} \frac{1}{2} \lambda x^2 & (x > 0) \\ \infty & (x = 0). \end{cases} \quad (7)$$

This is a truncated like potential. Truncation naturally arises due to the log term in the potential (5). When  $D$  increases, there is a transition from the Gaussian potential (6) to the truncated potential (7). The existence of two different shapes of potentials depending on the strength coupling  $D$  has implications in the probability distributions as we will show in the next section.

### 3.2 Probability Distribution

It is known that SPDE's can be generally transformed into Fokker-Planck equations (FK equations) which are mathematically equivalent to the original SPDE (See [18, 19, 20] for details). Then, we can transform Eq. (3) into the following FK equation:

$$\frac{\partial p(x, t)}{\partial t} = \frac{\partial}{\partial x} \{U'(x)p(x, t)\} + \frac{\sigma^2}{2} \frac{\partial^2}{\partial x^2} \{p(x, t)\}. \quad (8)$$

By solving this FK equation, the stationary distribution is given by

$$\begin{aligned} p(x) &= K \exp\left(-\frac{2}{\sigma^2}U(x)\right) \\ &= K \exp\left(\frac{2}{\sigma^2}\frac{A}{D} \log(C + Dx) - \frac{\lambda}{\sigma^2}x^2\right), \end{aligned} \quad (9)$$

where  $K$  is a normalization constant. Again, we can analyze the weak and strong coupling of unbounded transcriptional factors and gene operator site as follows.

**The weak coupling limit** In the weak feedback region,  $D \rightarrow 0$ , the probability distribution (9) reads as

$$p(x) = \sqrt{\frac{\lambda}{\sigma^2\pi}} \exp\left(-\frac{\lambda}{\sigma^2}\left(x - \frac{A}{\lambda C}\right)^2\right). \quad (10)$$

This is a Gaussian distribution.

**The strong coupling limit** In the strong feedback region  $D \rightarrow \infty$ , the distribution (9) changes and takes the form

$$p(x) = \begin{cases} 2\sqrt{\frac{\lambda}{\sigma^2\pi}} \exp\left(-\frac{\lambda}{\sigma^2}x^2\right) & (x > 0) \\ 0 & (x \leq 0). \end{cases} \quad (11)$$

This distribution corresponds to the truncated potential (7). It is worth noticing that this truncated distribution emerges as a consequence of the truncated potential (7). Next, in order to investigate the role of noise in the FBL module, we compute the expectation and variance values in both coupling limits.

### 3.3 Expectation value

The expectation value of gene expression level in the auto regulatory module is given as

$$E(D) = \langle x \rangle = \int_{-C/D}^{\infty} xp(x)dx. \quad (12)$$

The numerical solution of this expression is shown in Fig. 1. We observe two different states depending on the feedback strength  $D$ . In particular, we see a transition from high to low expectation values with increasing the feedback strength  $D$ . While it is difficult to obtain the analytical expression for all  $D$ , we can derive these two states by computing Eq. (12) in the coupling limits.

**The weak coupling limit** In the weak feedback region  $D \rightarrow 0$ , the expectation value (12) is given by<sup>1</sup>

$$E(D = 0) = \frac{A}{\lambda C}. \quad (13)$$

**The strong coupling limit** In the strong feedback region  $D \rightarrow \infty$ , the expectation value (12) reads

$$E(D = \infty) = \frac{\sigma}{\sqrt{\lambda\pi}}. \quad (14)$$

This is the expectation value corresponding to the truncated potential. It is particularly clear on this result that, in the strong coupling limit, the abundance of unbounded regulating protein is caused by the noise  $\sigma$ . In Fig. 1, we see that even in the strong feedback coupling region  $D$  (strongly self-repressed gene), there is a non-zero basal amount of proteins that emerges in our approach from the stochastic noise. In addition, it is worth noticing that deterministic analyses could not detect this protein concentration.

### 3.4 Variance

Next, we investigate the variance of gene expression level in FBL. Previous studies [12] have shown that variance of gene expression is strongly reduced in FBL modules. However here, as a main result we find here that, in the

---

<sup>1</sup>Here we write  $E(D = 0)$  instead of  $E(0)$  for highlighting the variable  $D$ .

strong coupling region, the feedback loop decreases the transcriptional noise in almost a 30 % more than described in previous studies. First, the variance is defined as

$$V(D) = \langle (x - E(D))^2 \rangle = \int_{-C/D}^{\infty} (x - E(D))^2 p(x) dx. \quad (15)$$

Eq. (15) was simulated and the result is shown in Fig. 2 in continuous line. In contrast, in dashed lines shown in Fig. 2, we can see the function corresponding to  $1/S_r$  shown in [12]. Furthermore, we analytically evaluate the variance for both limiting coupling regions.

**The weak coupling limit** In the weak feedback region  $D \rightarrow 0$ , the variance (15) reads as

$$V(D = 0) = \frac{\sigma^2}{2\lambda}. \quad (16)$$

**The strong coupling limit** In the strong feedback region  $D \rightarrow \infty$ , the variance (15) is given by

$$V(D = \infty) = \frac{\sigma^2}{\lambda} \left( \frac{1}{2} - \frac{1}{\pi} \right). \quad (17)$$

**Comparison with previous studies** In [12], a ratio of the absolute values of stability of the unregulated to auto-regulated modules was used to compare both systems. This is based on the fact that a system with higher stability exhibits a lower variance in gene expression. An equivalent computation can be performed in our analysis by evaluating the ratio of variances at different coupling limits. In this case, a very weak coupling limit ( $D \rightarrow 0$ ) corresponds to the unregulated module considered in [12]. The ratio is computed as follows:

$$\frac{V(D = \infty)}{V(D = 0)} = \left( 1 - \frac{2}{\pi} \right) = 0.363. \quad (18)$$

This expression is equivalent to the inverse of the relative stability  $1/S_r$  (in the strong coupling region), shown in Eq. (3) of [12]. In [12], it was



found that this ratio takes the value 0.5. Therefore, we see that our analysis suggests that the variance of the gene expression in the strong coupling region is reduced further than expected (28% more) [12]. This can also be seen by comparing the continuous and dashed line shown in Fig. 2.

### 3.5 Coefficient of variation

It is important to consider a magnitude that combines the expectation value and the variance. The coefficient of variation  $C_V$  is a measure of dispersion of a probability distribution. It is useful for comparing the uncertainty between different measurements of varying absolute magnitude. It is defined as the ratio of the standard deviation to the mean. This magnitude is often called variability or relative standard deviation when the absolute value of the  $C_V$  is expressed as a percentage.

$$C_V(D) = \frac{\sqrt{V(D)}}{E} \quad (19)$$

Fig.3 shows the result of the simulation of Eq. (19) for three sets of parameters.

**The weak coupling limit** In the weak feedback region  $D \rightarrow 0$ , the coefficient of variation reads as

$$C_V(D = 0) = \frac{\sqrt{\lambda\sigma C}}{\sqrt{2A}}. \quad (20)$$

**The strong coupling limit** In the strong feedback region  $D \rightarrow \infty$ , the coefficient of variation follows

$$C_V(D = \infty) = \sqrt{\frac{\pi}{2} - 1} = 0.755. \quad (21)$$

We see that in the case of a very large feedback strength  $D$ , the coefficient of variation  $C_V$  takes the value 0.75. Interestingly, this expression is independent of parameters. Fig. 3 shows the result of the simulation of Eq. (19) for three different sets of parameters. In all cases, we observed the same behaviour. In weak coupling limit ( $D \rightarrow 0$ ),  $C_V$  can be reduced by decreasing noise  $\sigma$ . However, in the strong coupling limit, we cannot reduce  $C_V$ , even if we decrease the noise  $\sigma$ . This is because in the strong coupling limit, the

abundance of protein is linear in noise  $\sigma$ , which cancels the noise dependence coming from the standard deviation contribution. Therefore, in the strong coupling limit, the relative value of variation  $C_V$  can not be further reduced. In other words, no external parameters can disturb the system. Thus, a FBL system operating in the strong feedback region is robust.

On the other hand, it is worth noticing that values in the vicinity of 0.75 were experimentally observed in [16]. Three different negative feedback loops were designed and analyzed under different concentrations of anhydrotetracycline hydrochloride (aTc) ranging from 0 to 100 ng/ml. These aTc molecules inhibit the negative feedback loop. These chemicals play the same role as the strength of regulation  $D$  in our approach. At low aTc concentrations, the strength of the FBL is strong ( $D$  large). In contrast, high aTc concentrations correspond to low  $D$  values. Experimental results described in [16] show that at very low aTc concentrations (i.e.,  $D \rightarrow \infty$ ), the  $C_V$  is in the vicinity of 0.75, in agreement with our theoretical results.

### 3.6 Noise dependence

This system is characterized by two phases or regions depending on the strength of the self-repression coupling  $D$ . In strong coupling region, the role of noise is more relevant. We here address the issue of analytically assessing the role of noise in the FFL module. We define the following noise dependence  $N$ <sup>2</sup>

$$N(D) = \frac{E(D, \sigma) - E(D, 0)}{E(D, \sigma)}. \quad (22)$$

This value  $N(D)$  indicates the contribution of the noise effect  $\sigma$  to the abundance (expectation value) of protein. In the strong coupling region,  $N(D) = 1$ , therefore it indicates that the system is completely dominated by the noise in this region. In contrast, in weak coupling region,  $N(D) = 0$ . Then, the influence of the noise is very small in this limit. We showed the numerical solution in Fig. 4.

---

<sup>2</sup>In (12), we write  $E(D)$  for expectation. However, in this section, we write  $E(D, \sigma)$  for that, since the expectation also depends on  $\sigma$ .

## 4 Conclusions

There have been a series of studies and model developments in recent years towards an understanding of small functional units of cells. Among them, FBL is an interesting module with important implications for cell regulation and stability [12].

A major challenge addressed in this study consisted in embedding a stochastic approach into the structure of this FBL. This approach based on stochastic theory presents a number of advantages if compared with deterministic analyses. We summarize them as follows: (1) We were able to identify a bimodal activity depending of the strength of self-repression coupling  $D$ . (2) In the strong coupling region, the variance of the transcriptional noise was found to be reduced a 28 % more than described earlier [12]. (3) The contribution of the noise effect to the abundance of regulating protein becomes manifest when the coefficient of variation was computed. This value was independent of all parameters and in fair agreement with the experimentally observed values [16]. This result could have not been found using deterministic models. (4) Our analysis revealed that the autoregulation process is significantly induced by the intrinsic and external noise in the strong coupling region. In short, it means that the existence of inherent noise in FBL makes it possible to produce a basal amount of proteins even although the repression level  $D$  is very high.

Finally, it remains to be explored to which extent this stochastic analysis can be extended to the analysis of noise propagation in networks composed of several modules [14, 15], and even in larger gene networks, and more interestingly in which way these large-scale networks can increase the robustness and stability.

## References

- [1] Kaern, M. T.C. Elston, W.J. Blake, and J.J. Collins, 2005. Stochasticity in gene expression; from theories to phenotypes. *Reviews Genetics* 6, 451-464.
- [2] Swain, P.S., Elowitz M.B. and Siggia E.D. (2002). Intrinsic and extrinsic contributions to stochasticity in gene expression. *Proc. Natl. Acad. Sci. USA* 99, 12795-12800.

- [3] Kepler T.B. and Elston TC (2001) Stochasticity in transcriptional regulation: origins, consequences and mathematical representations. *Biophys. J.* 81, 3116-3136.
- [4] Chen, L., Wang, R., Zhou T. and Aihara K. (2005). Noise-induced cooperative behavior in multicell system. *Bioinformatics* 21, 2722-2535.
- [5] Gardner, T.S., C.R. Cantor and J.J. Collins, 2000. Construction of a genetic toggle switch in *E. Coli*. *Nature* 403, 339-342.
- [6] Paulsson J (2004). Summing up the noise in gene networks. *Nature* 427, 415-418.
- [7] Elowitz M.B., Levine A.J., Siggia E.D., Swain P.S. (2002). Stochastic gene expression in a single cell. *Science* 297, 1183-1186.
- [8] Austin D.W., Allen M.S., McCollum J.M., Dar RD, Wilgus J.R. and Simpson M.L. (2006) Gene network shaping of inherent noise spectra. *Nature* 439, 608-611.
- [9] Blake W.J., Kaern M, Cantor C.E., Collins J.J. (2003) Noise in eukaryotic gene expression. *Nature* 422, 622-637.
- [10] Raser J.M., OfShea E.K. (2004) Control of stochasticity in eukaryotic gene expression. *Science* 304:1811-1814.
- [11] Savageau MA (1974) Comparison of classical and autogenous systems of regulation in inducible operons. *Nature* 252: 546-549
- [12] Becskei, A. and L. Serrano, 2000. Engineering stability in gene networks by autoregulation. *Nature* 405, 590-593.
- [13] Rosenfeld, N., M. B. Elowitz, and U. Alon. 2002. Negative autoregulation speeds the response times of transcription networks. *J. Mol. Biol.* 323:785-793.
- [14] Pedraza J.M. and van Oudenaarden A. (2005). Noise propagation in gene networks. *Science* 307:1965-1969.
- [15] Hooshangi S., Thiberge S., Weiss R. (2005) Ultrasensitivity and noise propagation in a synthetic transcriptional cascade. *Proc. Natl. Acad. Sci. USA* 102:3581-3586.

- [16] Dublanche Y., Michalodimitrakis K., Kummerer N., Foglierini M. And Serrano L. (2006). *Mol. Systems Biology* 41, 1-12.
- [17] Wolf D.M. and F.H. Eeckman, 1998. On the relationship between genomic regulatory element organization and gene regulatory dynamics. *J. Theor. Biol.* 195, 167-186.
- [18] Wong, E., 1971. *Stochastic Processes in Information and Dynamical Systems*, Ed. New York, McGraw-Hill.
- [19] van Kampen, N.G., 1992. *Stochastic processes in physics and chemistry*, Elsevier Science B.V.
- [20] Mikosch, T., 1998. *Elementary Stochastic Calculus with Finance in View*, World Scientific Publishing Co. Pte. Ltd.
- [21] T. Ochiai, J.C. Nacher, T. Akutsu, *Physics Letters A* 330 (2004) pp.313.
- [22] T. Ochiai, J.C. Nacher, T. Akutsu, *Physics Letters A*, 339 (2005) pp.1.

### Expectation of gene expression level

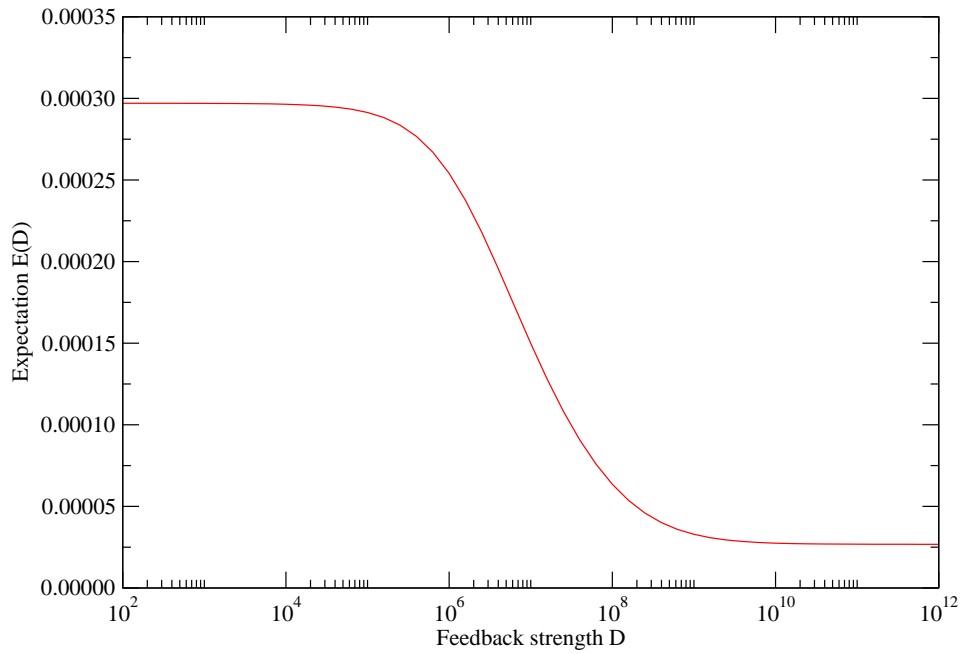


Figure 1: We show the expectation value of gene expression level in the auto-regulatory genetic module. Horizontal axis denotes feedback strength  $D$  and vertical axis denotes the expectation value of gene expression level  $E(D)$ . The numerical values of the system parameters are taken from [12]:  $A = 4.5 \times 10^{-6} [\text{Ms}^{-1}]$ ,  $C = 1.5 \times 10^3$ ,  $\lambda = 10^{-5} [\text{s}^{-1}]$ , and  $\sigma = 1.5 \times 10^{-7} [\text{Ms}^{-1/2}]$  is an arbitrary parameter.

### Variance of gene expression level

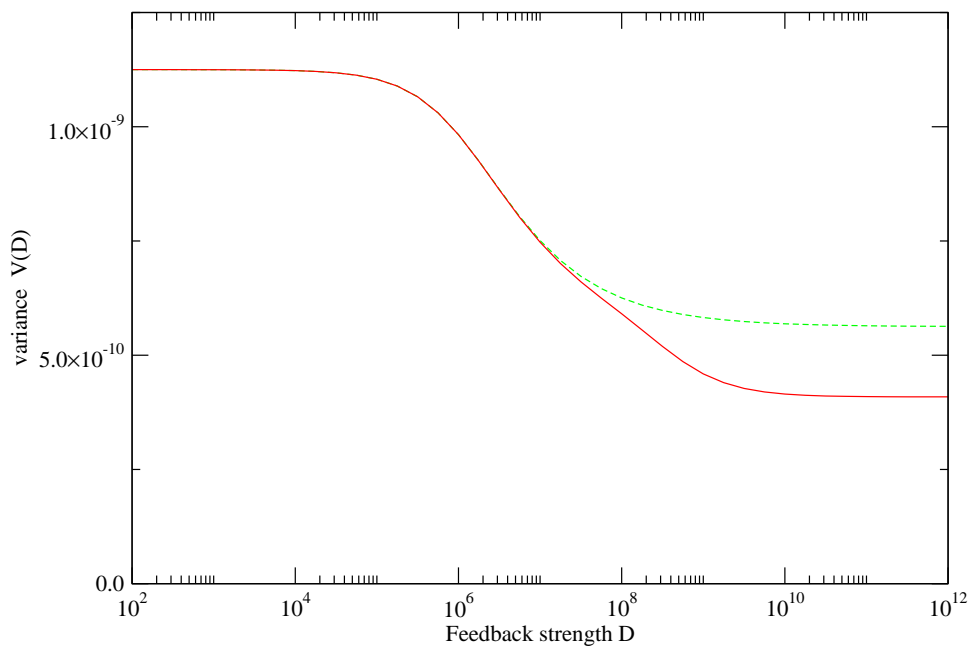


Figure 2: We show the variance of gene expression level in the auto-regulatory genetic module. Horizontal axis denotes feedback strength  $D$  and vertical axis denotes the variance  $V(D)$ . The continuous line is our result and the dashed line is the result from [12]. We see that the variance in the gene expression is reduced further than expected (28% more) in the strong coupling region. The numerical values of the system parameters are the same as Fig. 1.

### Coefficient of Variation

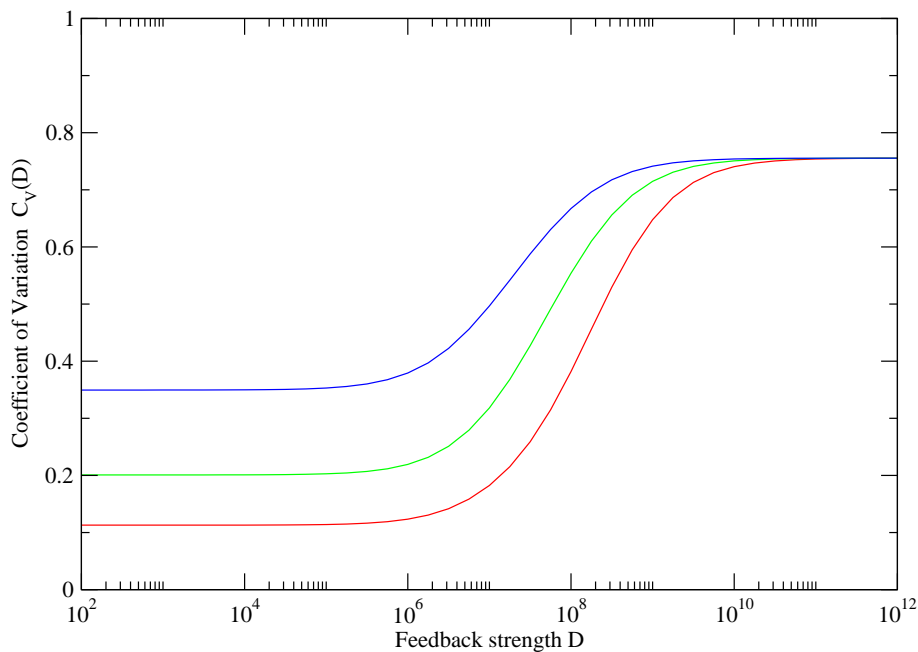


Figure 3: We show the coefficient of variation (standard deviation/mean). Horizontal axis denotes feedback strength  $D$  and vertical axis denotes the coefficient of variation  $C_V$  (standard deviation/mean). The numerical values of the system parameters are the same as Fig. 1. but noise size  $\sigma$  takes the following values. red curve  $\sigma = 1.5 \times 10^{-7} [\text{Ms}^{-1/2}]$ , green curve  $\sigma = 1.5 \times 10^{-6.75} [\text{Ms}^{-1/2}]$ , and blue curve  $\sigma = 1.5 \times 10^{-6.5} [\text{Ms}^{-1/2}]$ . In the strong feedback region, all three curves go to the same value 0.755



### Noise dependence

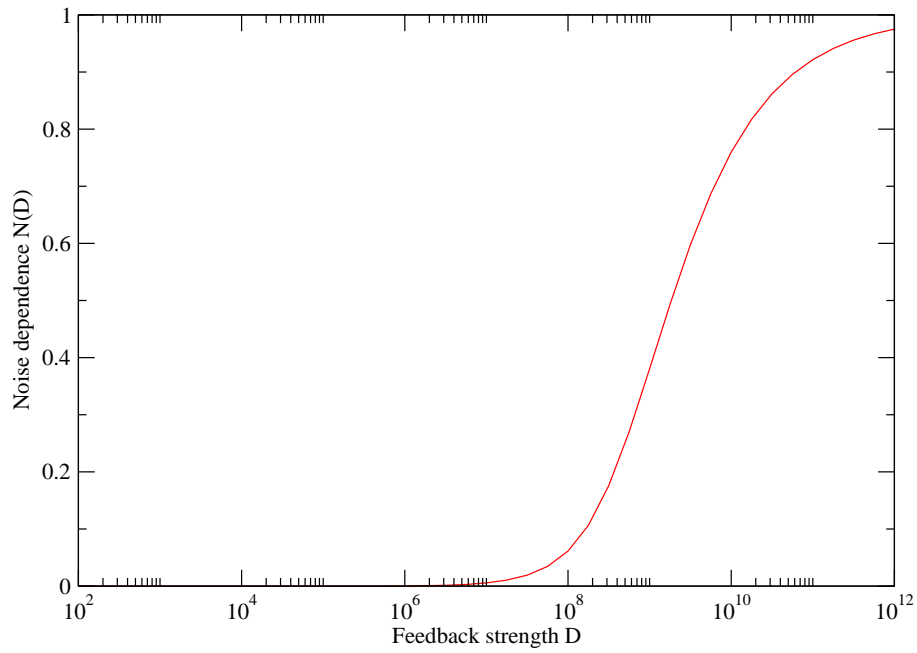


Figure 4: We show the noise dependence  $N(D)$ . Horizontal axis denotes feedback strength  $D$  and vertical axis denotes the noise dependence  $N(D)$ . The numerical values of the system parameters are the same as Fig. 1.